

# 1 Dissolved oxygen as indicator of multiple drivers of the marine 2 ecosystem: the Southern Adriatic Sea case study

3 Valeria Di Biagio<sup>1</sup>, Riccardo Martellucci<sup>1</sup>, Milena Menna<sup>1</sup>, Anna Teruzzi<sup>1</sup>, Carolina Amadio<sup>1</sup>, Elena  
4 Mauri<sup>1</sup>, Gianpiero Cossarini<sup>1</sup>

5 <sup>1</sup>National Institute of Oceanography and Applied Geophysics - OGS, Trieste, Italy

6 *Correspondence to:* Valeria Di Biagio (vdibiagio@ogs.it)

7 **Abstract.** Oxygen is essential ~~for~~ all aerobic organisms and its dynamics in the ocean involve interconnected physical and  
8 biological processes that are at the basis ~~of~~ the marine ecosystem functioning. ~~The study Investigation~~ of dissolved oxygen  
9 (DO) variations under multiple drivers is currently one of the main goals of climate and marine ecological scientific  
10 communities, ~~and these well as~~ ~~quantification of~~ ~~DO levels~~ is essential for the assessment of the environmental status,  
11 especially in ~~the~~ coastal areas.

12 We investigate the 1999-2021 interannual variability of DO in the ~~s~~Southern Adriatic Sea, a marginal area of the Mediterranean  
13 Sea, ~~where hosting~~ deep water formation processes ~~occur, that significantly~~ ~~contributing significantly~~ to the ventilation of the  
14 Eastern Mediterranean basin. Following the Marine Strategy Framework Directive, ~~which that~~ promotes the integration of  
15 different observational platforms, we use DO modelled by the ~~latest~~ Copernicus Marine ~~Mediterranean Sea~~ biogeochemical  
16 reanalysis, ~~which that~~ assimilates satellite chlorophyll ~~concentrations~~ and ~~to~~ which we apply a bias correction ~~by~~ using DO  
17 Argo float measurements in 2014-2020. A correlation analysis of the ~~time series of the~~ first three modes of variability (86%  
18 of ~~the total explained~~ variance) of the DO profiles extracted from the bias-corrected reanalysis with key meteo-marine  
19 indicators ~~show reveals~~ a link (~~r>0.4~~) with (i) net heat fluxes related to oxygen solubility, (ii) vertical mixing, (iii) biological  
20 production at ~~the surface and in~~ subsurface layers, and (iv) circulation associated ~~with the~~ entrance of northern Adriatic  
21 waters ~~as interrelated drivers~~. The alternating entrance of Levantine ~~and Modified~~ Atlantic Waters through the North Ionian  
22 Gyre (NIG) appears ~~to be~~ the driver of the fourth mode of variability, ~~which that~~ explains 8% of ~~the total~~ variance. Moreover,  
23 we find that the first temporal mode of variability is the main ~~drive contributor~~ of the ~~2021~~ negative anomaly of DO in the 0-  
24 600 m layer ~~in 2021~~ with respect to the 1999-2020 climatology. We ascribe the lower content of DO in 2021 to a negative  
25 anomaly of the subsurface ~~biological~~ production in the same year, in agreement with the previous correlation analysis, but not  
26 to heat fluxes. ~~Indeed, fact,~~ in agreement with previous studies, we observe ~~a sharp increase the in entrance of warmer and~~  
27 ~~exceptionally~~ ~~salinity~~ ~~water~~ favoured by the cyclonic circulation of NIG from 2019 onwards. We interpret ~~this~~ as a  
28 possible regime shift ~~that is~~ not captured by the time series analysis, ~~and~~ whose possible consequences ~~for~~ Ionian-Adriatic  
29 system ventilation and ~~for~~ marine organisms should be carefully monitored in the near future.

## 30 1 Introduction

31 Dissolved oxygen (DO) is a key indicator ~~for~~ monitoring the marine ecosystem functioning, ~~because~~ it is the result of  
32 several atmospheric, hydrodynamical and biogeochemical driving processes (~~such as~~, air-sea fluxes, vertical convection  
33 and mixing, horizontal transport, biological production and consumption; Keeling and Garcia, 2002; Oschlies et al., 2018;  
34 Pitcher et al., 2021). Indeed, DO is currently ~~being studied~~ investigated under the global warming scenarios by climate and marine  
35 ecological scientific communities (e.g. ~~Pörtner et al., 2019~~; Kwiatkowski et al., 2020; Garcia-Soto et al., 2021), as oxygen  
36 depletion has been observed ~~in both at level of~~ the global ocean as ~~well as~~ at local scale (Breitburg et al., 2018). Climate  
37 models predict a ~~future~~ reduction in global ocean dissolved oxygen content (Matear et al., 2000; Oschlies et al., 2008; Stramma  
38 et al., 2010, Reale et al., 2021), ~~so making~~ this parameter ~~is~~ of primary interest especially in those areas where oceanic processes  
39 connect surface ~~with~~ deep layers.

40 ~~Despite being a marginal sea,~~ the ~~s~~Southern Adriatic Sea (SAdr, Fig. 1a) ~~is one of these areas~~ has a crucial importance for  
41 ~~the Eastern Mediterranean Sea ventilation,~~ ~~as~~ it is an area of deep water formation (Gačić et al., 2002; Pirro et al., 2022)  
42 ~~and represents the deep engine of the eastern Mediterranean thermohaline circulation (Malanotte-Rizzoli et al., 1999), which~~  
43 ~~is crucial for the eastern basin ventilation.~~

44 The Adriatic Sea (Fig. 1a) is an elongated, semi enclosed and ~~roughly~~ approximately north-to-south oriented basin characterized  
45 by a shallow northern shelf (~~depth~~ shallower than 80 m) and a deep pit in its southern part (maximum depth of ~~f~~ approximately ~~over~~  
46 1200 m) which is connected to the Ionian Sea (central Mediterranean basin) through the Otranto Strait (with ~~a~~ maximum depth  
47 of 800 m). The Adriatic Sea is characterized by a cyclonic circulation governed by several drivers: river runoff, wind stress,  
48 surface buoyancy fluxes and mass exchanges through the Otranto Strait (Cushman-Roisin et al., 2013).

49 ~~Being at the connection between Ionian and Adriatic Sea,~~ the SAdr is strongly influenced by the seawater exchange with the  
50 ~~Northern Adriatic Sea and by the inflow of Levantine and/Modified Atlantic Waters under the alternate Northern Ionian Gyre~~  
51 ~~circulation (Menna et al., 2019) and shows an intermittent pattern of surface phytoplankton blooms (Gačić et al., 2002;~~  
52 ~~Civitarese et al., 2010).~~ The SAdr is strongly influenced by the inflow of water masses from the northern Adriatic Sea (i.e.,  
53 ~~North Adriatic Dense Water, Querin et al., 2016) and the Ionian Sea. In particular, the inflow of southern water masses is~~  
54 ~~triggered by the periodic reversal of Northern Ionian Gyre circulation (Gačić et al., 2002; Civitarese et al., 2010, Menna et al.,~~  
55 ~~2019). This oscillating system, called the Adriatic - Ionian Bimodal Oscillating System (BiOS), changes the circulation of the~~  
56 ~~Northern Ionian Gyre from cyclonic to anticyclonic and vice versa, modulating the advection of water masses in the Adriatic~~  
57 ~~Sea (Gačić et al., 2010, Rubino et al., 2020). The cyclonic circulation of the Northern Ionian Gyre causes the advection of~~  
58 ~~saline water masses of Levantine origin (i.e., Levantine Intermediate Water, Cretan Intermediate Water, Ionian Surface Water~~  
59 ~~and Levantine Surface Water, Manca et al., 2006), while the anticyclonic circulation favours the inflow of Atlantic water and~~  
60 ~~a relative decrease of salinity in the SAdr (Gačić et al., 2011, Menna et al., 2022a). This feature has a strong influence on the~~  
61 ~~biogeochemical properties of the SAdr, affecting nutrient availability (Civitarese et al., 2010), phytoplankton blooms (Gačić~~  
62 ~~et al., 2002; Civitarese et al., 2010), and species composition (Batistić et al., 2014, Mauri et al., 2021).~~

63

64 While hydrodynamic~~al~~ and biogeochemical properties of SAdr have been widely described ~~by~~in several studies (e.g.,  
65 Civitarese et al. 2010; Cushman-Roisin et al., 2013; Lipizer et al., 2014; Kokkini et al., 2018, 2019; Mavropoulou et al., 2020;  
66 Mihanović et al., 2021; Menna et al., 2022**b**), at the best of our knowledge DO dynamics in the area ~~in~~and their connection  
67 with relevant driving processes over decadal time scales have not been addressed yet.

68 Investigating the DO multidecadal variability ~~represents a~~is crucial ~~element t~~for quantifying the state of the marine  
69 environment (Marine Strategy Framework Directive, ~~sensu~~ MSFD; Oosterwind et al., 2016) and ~~f~~or understanding  
70 anthropogenic impacts on the marine environment (Pörtner et al., 2022). The emerging ecosystem-based management method  
71 proposed by the ~~Marine Strategy Framework Directive~~ (2008/56/EC) promotes the use of different observational~~al~~ platforms,  
72 allowing to synoptically collect information on the space-time distribution of ~~major~~ important parameters related to water  
73 quality (Martellucci et al., 2021).

74 In this context, the present work integrates the state-of-the-art approach of in-situ measurements (in 2014-2020, distributed  
75 by i.e., Copernicus In Situ TAC ~~data in 2014-2020~~) with the ~~latest released~~ Copernicus Mediterranean biogeochemical  
76 reanalysis in the Mediterranean Sea at high 1/24° horizontal resolution (Cossarini et al., 2021), with the aim of characterizing  
77 the DO dynamics in the SAdr in the 1999-2021 time period. In particular, we aim at assessing DO inter-annual variability in  
78 an area (SAdr) sensitive to multiple drivers (e.g., atmospheric forcing, Mediterranean circulation, and biological processes)  
79 and to evaluate the relative importance of the different drivers in this area.

## 80 **2 Data and methods**

81 In the present study the DO concentration in the SAdr area (Fig. 1a) ~~was~~been assessed by combining data from the Copernicus  
82 Mediterranean reanalysis in the Mediterranean Sea~~data~~ (Prod1 in Table 1; Cossarini et al., 2021) in 1999-2021 and the  
83 Copernicus in situ dataset (Prod2, <https://doi.org/10.13155/75807>), available ~~forever~~in the time period 2014-2020 (Figs. 1b-  
84 c). The temporal evolution of the combined model-in situ DO concentration profile in 1999-2021 time period is shown in Fig.  
85 1d.

86 In particular, we used the BGC-Argo float measurements of in situ DO ~~provided by the~~ CMEMS In Situ TAC catalog  
87 to compute a bias correction to the daily DO concentrations~~s~~ simulated by the ~~Copernicus Marine~~ biogeochemical  
88 Mediterranean reanalysis at 1/24° horizontal resolution. In fact, the biogeochemical reanalysis does not include BGC-Argo  
89 float DO assimilation and displays an average RMSD of 15 mmol m<sup>-3</sup> for DO in the 0-600 m depth layer with respect to the  
90 observations in the area (Cossarini et al., 2021, Teruzzi et al., 2021a-b). Quantile Mapping, a technique largely used for  
91 climate simulations (e.g., Hopson and Webster, 2010; Themeßl et al., 2011; Gudmundsson et al., 2012), was adopted to perform  
92 the reanalysis bias correction. The Quantile Mapping technique adjusts the cumulative distribution of the data simulated  
93 for the past or future period by applying a transformation between the quantiles of the simulated and observed data in the at  
94 present. In our application, we adapted the code publicly provided by Beyer et al. (2020) at

95 <https://doi.org/10.17605/OSF.IO/8AXW9> and included ~~considered the distribution of~~ available *in situ* data of daily DO (Fig.  
96 1c) within a representative area (Fig. 1b) of the southern Adriatic in the period 2014-2020, and DO reanalysis data for the same  
97 days of measurements.

98 ~~Then, we applied the estimated quantile transformation between the two data sets to the whole 1999-2021 reanalysis time~~  
99 ~~series, by adapting the code publicly delivered by Beyer et al. (2020) at <https://doi.org/10.17605/OSF.IO/8AXW9>.~~ The  
100 representative area ~~was~~ identified by applying a spatial ~~cross-auto~~correlation analysis (Martellucci et al., 2021) ~~to~~ the  
101 biogeochemical reanalysis centered on the SAdr pit and selecting the correlation threshold of 0.9 (Fig. 1b). Specifically, we  
102 considered the cross-correlation between the surface data of DO, nitrate and chlorophyll concentrations in the central point of  
103 the pit and those at each spatial grid point in the domain, to identify the area that displayed the same dynamics at the surface  
104 from a phenomenological perspective. ~~The temporal evolution of the combined model-*in situ* DO concentration profile in~~  
105 ~~1999-2021 time period used in the following analysis is reported in Fig. 1d. Further details on the Quantile Mapping bias~~  
106 ~~correction are included in Appendix A.~~

107 We then applied the Empirical Orthogonal Function (EOF) analysis (e.g. Thomson and Emery, 2014) to the vertical profiles  
108 in Fig. 1d ~~in order~~ to describe ~~the~~ DO variability in the SAdr area in the period 1999-2021. The EOF analysis allows us to  
109 identify the ~~spat~~vertical patterns of variability (i.e., ~~EOF vertical patterns~~spatial modes), ~~to~~ describe how they change in time  
110 by means of time series (i.e., ~~EOF time series~~temporal modes), and ~~to~~ associate the explained variance ~~with~~ each  
111 ~~mode~~pattern.

112 Finally, we ~~performed~~ conducted a Pearson correlation analysis between the EOF ~~time~~temporal seri modes in 1999-2021 and the  
113 following series of forcing indexes (reported in Fig. 2) providing evidence of the mechanisms driving ~~the~~ oxygen concentration  
114 and dynamics in the area:

- 115 - heat fluxes in the SAdr as a proxy for thermal and mixing ~~and~~ /stratification cycles (from Prod3; Fig. 2a);
- 116 - ~~the~~ mixed layer depth in the SAdr as a proxy for both local vertical mixing and water residence times in the pit (Prod3; Fig.  
117 2b);
- 118 - chlorophyll concentration at surface and in- at subsurface ~~level~~ in the SAdr as a proxy for biological production in spring and  
119 late spring-summer, respectively (Prod1; Fig. 2c-d);
- 120 - heat fluxes in the northern Adriatic Sea (NAdr), as a proxy for dense water oxygen-rich formation in the NAdr and its  
121 transport into the pit (Prod3; Fig. 2e);
- 122 - Northern Ionian Gyre (NIG) vorticity derived from satellite altimetry, as a proxy of the inflow of Levantine waters and  
123 ~~Modified~~ Atlantic Water (MAW) (Prod4 and Prod5; Fig. 2f).

124 In particular, the temporal phases of the NIG are defined as cyclonic and anticyclonic, respectively, when the vorticity field is  
125 positive and negative, as highlighted by the de-seasonalized time series in Fig. 2f.

126 Mixed layer depth (computed in Prod3 considering the 0.03 kg m<sup>-3</sup> density difference with respect to the near-surface value at  
127 10 m depth) ~~and~~, the chlorophyll at surface and in subsurface ~~level~~ (30-80 m, where ~~hosting~~ the deep chlorophyll maximum is  
128 located~~feature~~), were spatially averaged in the SAdr area (41.6°-42.1°N; 17.6°-18.1°E), to consider the whole volume of the

129 pit); heat fluxes were calculated in both the SAdr area and in the NAdr area (44.5°-45.5°N; 13°-13.5°E), while current vorticity  
130 was computed in the Northern Ionian Sea (37°-39°N; 17°-19.5°E).  
131 In the correlation analysis, the time series of the heat fluxes in NAdr Sea (Fig. 2e) has been temporally lagged by 2 months, as  
132 an estimated mean time for the entrance in the SAdr pit of waters originated in the Northern Adriatic area (Vilibić et al., 2013;  
133 Querin et al., 2016; Mihanović et al 2021). Moreover, we tested the significance of the correlation coefficients between EOF  
134 and driver time series using a parametric t-test (with a reference significance level of 0.05). The current vorticity in the Northern  
135 Ionian area in Fig. 2f has been previously filtered by a low-pass filter of 13 months. The temporal phases of the NIG are defined  
136 as anticyclonic when the vorticity field is negative and cyclonic when the vorticity field is positive.

## 137 3 Results

### 138 3.1 Temporal scales of variability in connection with drivers EOF analysis

139 Dissolved oxygen in the southern Adriatic area (Fig. 1a) shows in the subsurface layers an alternation between periods of  
140 enrichment (in 2004-2006, 2010-2013, 2016-2017) and sharp declines that impacted the Oxygen Minimum Layer (OML),  
141 located between 100 and 300 m. Low concentration values are observed also in the years between 1999 and 2003.

142 The EOF analysis was performed on the vertical profiles of the oxygen anomaly, derived by removing the mean profile in the  
143 period 1999-2021, and then normalized dividing by their standard deviation.

144 The time series temporal evolution of the first four EOF modes, which explain up to 95% of the oxygen variability in the water  
145 column are shown, along together with the corresponding verspatial patterns, are reported in Figs. 3a,c,e,g and Figs. 3b,d,f,h  
146 (left and right columns, respectively).

### 147 3.2 Temporal scales of variability in connection with drivers

148 The interpretation of the EOFs are interperformed considering the correlation of the EOF time temporal serimodes (first  
149 column of Figs. 3a,c,e,g) with the time series of the forcing indicators shown reported in Fig. 2 (see Table 2), with heat fluxes  
150 in the nNorthern Adriatic Sea time-lagged by two months as the estimated time of entry of the NAdr dense water to enter in  
151 the SAdr pit.

152 The first temporal mode (Figs. 3a-b), that accountings for 48.9almost the 50% of the explained variance, can be associated  
153 with to the seasonal cycle of the oxygen concentration in the upper layers: its vertical pattern mainly affects the first levels (Fig.  
154 3b), the corresponding time series shows relative maximum values in spring (Fig. 3a); it influences mainly the first vertical  
155 levels (Fig. 3b) and it shows a statistically significant but moderate correlation is significantly correlated (r=0.56) with the heat  
156 flux and a lower correlation with the subsurface chlorophyll concentration (r=0.43) in the SAdr area (first column in Table 2).

157 The second and the third temporal modes (Figs. 3c-d and 3e-f, respectively), which describe 19.7% and 17.7%  
158 approximately 20% of the variance respectively each, affect influenced both the upper and the deeper layers. Both modes display  
159 relative maximum values in summer, but they have different correlation coefficients with the explanatory mining facto drivers.

160 The time series of the second mode (second column in Table 2) shows a significant but low correlation with multiple drivers,  
161 exceeding 0.4 only for surface chlorophyll ( $r=-0.41$ ) and waters from the NAdr area ( $r=0.48$ ). The time series of the third mode  
162 (third column, same Table) is moderatestrongly correlated with both surface chlorophyll ( $r=-0.61$ ) and NAdr waters ( $r=0.68$   
163 correlation), but also with heat fluxes in the area ( $r=0.51$ ), and, to a lower extent, with mixed layer depth ( $r=-0.41$ ) and  
164 subsurface chlorophyll ( $r=0.48$ ).

165 The fourth mode (Figs. 3g-h), ~~that despite disdescribes~~ plays less than 8-10% of the variance, can be ~~mainly~~-ascribed mainly to  
166 the vorticity of the NIG ( $r=-0.3744$ , last column in Table 2), which ~~affect~~influencees the oxygen concentration in the  
167 intermediate layer (100-500 m depth), filled by LIW, and acts in the opposite direction in the upper and deeper layers (Fig.  
168 3h).

169 Analysing the four modes in order of decreasing explained variance, we ascribeWhile the ~~first mode explains the variability~~  
170 ~~(e.g. seasonal variability)~~ connected with solubility mainly to the first mode, whereas we associate the biological contribution  
171 to oxygen dynamics ~~is ascribed~~ to multiple interacting modes. ~~In fact, t~~The first mode explains the onset of the subsurface  
172 oxygen maximum (SOM) in spring, while the summer dynamics of the SOM is partially related to the third mode. The second  
173 ~~modeEOF~~, whose time series is correlated with the surface chlorophyll evolution among other factors, can explain that part  
174 of the oxygen variability that is relatlinked to ~~the~~-winter surface productivity.

175 The SOM, ~~recognisable~~vident in summer oxygen profiles in Figs. 1c-d at ~~about~~approximately 40 m depth, is a feature that has  
176 already been observed in a great part of oligotrophic oceans (Riser and Johnson, 2008; Yasunaka et al., 2022) and of the  
177 Mediterranean Sea (e.g., Kress and Herut, 2001; Copin-Montégut and Bégovic, 2002; Manca et al., 2004; Cossarini et al.,  
178 2021; Di Biagio et al., 2022) and it ~~represente~~constitutes an emerging property resulting from ~~multipleseveral~~ interacting  
179 ecosystem processes (i.e., air-sea interactions, transport, mixing and biological production and ~~/~~consumption) and is, indeed,  
180 captured by multiple modeEOFs.

181 The third mode, which also describes the high concentration values in the deep layers in the period 2005-2006 and 2012-2014,  
182 ~~seem~~ is also moderatestrongly associateconnected with a multi-annual signal of the inflow of deep denser and oxygenated water  
183 from the northern Adriatic Sea ( $r=0.68$ , third column in Table 2; Querin et al., 2016). Finally, it is worth ~~to-noting~~e that an  
184 EOF analysis ~~done-of-in-the~~ detrended DO time series (not shown) yieldprovides fairlpretty similar results but with the third  
185 mode only weakly correlated with the forcing indexes ( $r<0.4$ ). Indeed, we can conclude that the third mode captures a signal  
186 of long-term evolution of oxygen concentration ~~associa~~connected with changes in heat fluxes and chlorophyll concentration.

### 187 **3.23 The 2021 anomaly**

188 The year 2021 shows an overall negative anomaly in the oxygen concentration profile (Fig. 4b) comparedwith ~~respect~~ to the  
189 1999-2020 climatological profiles (Fig. 4a). In particular, the anomaly affecinterests a layer that ~~became~~-thinned~~d~~r during the  
190 year, moving from 0-600 m depth in winter-early spring season, to 30-400 m in late spring-summer and 0-80 m in fall. The  
191 (absolute) mMaximum ~~(absolute)~~-values correspond to 25-30 mmol m<sup>-3</sup> at the surface in spring and at the SOM depth in  
192 summer.

193 We verified that, among the EOF ~~modes~~, the negative anomaly of the first ~~EOF temporal~~-mode is the main contributor ~~tfor~~ the  
194 2021 negative oxygen anomaly (not shown). The ~~time series of the first EOF temporal~~-mode (Fig. 3a) is actually negative  
195 from 2019; and ~~it corresponds to the negative is correlated with the~~ anomaly of only one of its drivers (Table 2), i.e., ~~lower-~~  
196 ~~than average~~-subsurface chlorophyll (Fig. 2d), and not heat fluxes (Fig. 2a). ~~In particular, we estimated a mean negative~~  
197 ~~anomaly approximately equal to 6% with respect to the climatological mean (1999-2020) for subsurface chlorophyll in 2021.~~  
198 ~~One of the causes of the decrease in total oxygen concentration in the SAdr could be due to the exceptional salinization~~  
199 ~~observed in the SAdr since 2017 (Mihanović et al., 2021, Menna et al., 2022b). Additionally, the 2021 negative anomaly of~~  
200 ~~oxygen profile seems also to be connec~~This increase was related to the ~~inflow entrance~~-of new ~~water masses~~, warmer and  
201 noticeably saltier ~~water masses~~, from the ~~-northeastern Ionian Sea~~-Levantine basin, starting from the end of 2019. (Mihanović  
202 et al., 2021, Menna et al., 2022b).), for which the temperature reached 15–16°C at 100–800 m depth and salinity 39–39.1 psu  
203 at 100–200 m, 38.9–39.0 psu at 200–800 m in the SAdr area (not shown). ~~The inflow of~~ Indeed, the NIG, which shows a positive  
204 ~~vorticity since 2019, transported~~ saltier and warmer water masses is also evident by observing the temporal evolution of these  
205 parameters through the Strait of Otranto (Fig. B1). In particular, in the upper layer (0–150 m) both temperature and salinity  
206 show an overall positive trend throughout the period 1999–2021, whereas the decrease observed in 2006–2011 and 2017–2018  
207 can be associated with the inflow of less saline AW, triggered by the anticyclonic circulation of the NIG (Fig. 2f). In the  
208 intermediate layer (150–600 m), salinity shows a positive trend in 1999–2021, while no clear trend is observed for temperature.  
209 Moreover, a sharp increase in salinity (~ 0.1) is observed in 2019. This increase occurred after the NIG inversion from  
210 anticyclonic to cyclonic (Fig. 2f), resulting in a further increase in salinity due to both the decrease in AW advection and the  
211 increase in LIW inflow toward the Adriatic Sea (Mihanović et al., 2021) than during the two previous positive periods (1999–  
212 2005 and 2010–2016).

#### 213 4 Conclusions

214 ~~M~~The merging of the ~~latest~~ Copernicus biogeochemical reanalysis in ~~the~~ Mediterranean Sea with *in situ* TAC data of  
215 biogeochemical Argo floats allowed ~~us~~ to characterize the interannual variability of dissolved oxygen in the Southern Adriatic  
216 Sea in the 1999–2021 time period ~~and the 2021 anomaly with respect to the mean over 1999–2020~~. This study enriches our  
217 knowledge ~~abofut~~ the dissolved oxygen state and long-term dynamics in the area, by proposing a seamless time and space  
218 perspective that is complementary to previous climatologies and data aggregation information (e.g. Lipizer et al., 2014) and  
219 adding an explanatory framework ~~for~~ the driving mechanisms ~~in~~ the marine environment.

220 The EOF statistical analysis ~~that~~ we conducted on the vertical oxygen profiles ~~yield~~showed two ~~key~~main results. Firstly, in  
221 contrast with a climatological view, the analysis ~~was~~ been able to capture most of the inter-annual oxygen variability  
222 ~~associated in connection~~ with ~~the~~-variability of the main drivers (i.e., heat fluxes ~~affect~~influencing solubility; biological  
223 productivity; vertical mixing). We do not ~~detect~~ recognise a clear deoxygenation trend in the subsurface layer, while the  
224 multiannual variability is characterized by an ~~sort of alternation~~ cycle of enrichment and reduction phases, whose dominant

225 correlations with the drivers for each EOF ~~time series temporal mode~~ are found in the (absolute) range 0.40-0.70. The  
226 ~~possibility to observe evidence of~~ such cyclic signals is enhanced by the relatively small volume and short residence time of  
227 the SAdr pit waters (Querin et al., 2016) with respect to other Mediterranean areas (Coppola et al., 2018).  
228 This feature makes the SAdr a potential efficient probe to detect a ~~rapidfast~~ response to ~~long-term~~ changes in its meteo-marine  
229 drivers, i.e., circulation and atmospheric patterns.  
230 Indeed, as our second result, the variability that is not explained by the EOF decomposition appears to be connected with a  
231 possible regime shift, associated with the entrance of new water masses, warmer, markedly saltier and less oxygenated, that  
232 were not previously observed in the analyzed time period.  
233 The exceptional increase in salinity occurring after 2019 has been already documented (Mihanović et al., 2021; Menna et al.,  
234 2022b) and also observed ~~also~~ north of the SAdr pit. ~~FurtherContinuing the~~ monitoring of such anomalously high salinity  
235 values and ~~assessment ofing~~ their potential impact on the marine food web is of great importance, ~~assinee~~ picoplankton groups  
236 are sensitive to this environmental variable (Mella-Flores et al., 2011) and changes in biomass and production due to salinity  
237 have ~~been~~ already been observed in previous studies in the Adriatic Sea (Beg Paklar et al., 2020; Mauri et al., 2021). Moreover,  
238 if such a strong negative oxygen anomaly as observed in 2021 ~~were to~~ persist, it could have direct ~~impacte~~ consequences on  
239 local marine organisms, as well as on the cycling of dissolved chemical elements (Conley et al., 2009) potentially altering the  
240 energy flux towards the higher trophic levels (Ekau et al., 2010). ~~Indeed, t~~The importance of the relationship between ~~the~~  
241 dissolved oxygen and the catch distribution of some marine species has already been proved in the Adriatic Sea (Chiarini et  
242 al., 2022).  
243 ~~Our study, b~~By integrating model and *in situ* data, our study demonstrates the importance of following up the oxygen content  
244 in a seamless spatial and temporal way, ~~assinee~~ it is a fundamental indicator of good environmental status (GES, Oesterwind  
245 et al., 2016) and a factor that significantly ~~affect~~s fishing activities and economy.

## 246 247 **Appendix A: Quantile Mapping bias correction of DO concentration profiles**

248 Figures A1 and A2 show the modelled DO concentration profiles and histogram distributions before and after the Quantile  
249 Mapping bias correction, respectively, conducted by using the BGC-Argo float measurements available in 2014-2020 (Fig.  
250 1c). The Quantile Mapping, better than other methods (i.e. Additive Delta Change, Multiplicative Delta Change and Variance  
251 Scaling; results not shown), acted on the profiles by modifying the values of the concentrations (as indicated by the different  
252 colorbars in Figs. A1a and A1b) but, at the same time, maintaining the main dynamics observed before the correction: mixing  
253 and stratification at the surface during the year, subsurface oxygen maximum onset in spring and development in summer, and  
254 interannual variability related to the mixed layer depth dynamics in the intermediate layers. The distributions of the values of  
255 the model output before and after the Quantile Mapping bias correction and the values from BGC-Argo floats are displayed in  
256 Fig. A2. The correction actually changed the modelled values (Fig. A2a) to reproduce the shape of the distribution of the  
257 observations (Fig. A2c). In particular, after the correction (Fig. A2b) the modelled data show higher variability and a more  
258 skewed distribution toward the higher values, similarly to the observations.

259

260 **Appendix B: Time series of surface and intermediate temperature and salinity at the Otranto Strait**

261

262 **Data availability**

263 Publicly available datasets were analyzed in this study. Modelling and *in situ* data can be found at the Copernicus Marine  
264 Service, with references and DOIs indicated in the Table 1 of the manuscript.

265

266 **Author contribution**

267 VDB and GC conceived the idea. VDB, RM and MM conducted the analysis. VDB, RM and GC wrote the first draft, with  
268 contributions from the other co-authors. All the authors discussed and reviewed the submitted manuscript.

269

270 **Competing interests**

271 The authors declare that they have no conflict of interest.

272

273 **Acknowledgements**

274 This study has been conducted using EU Copernicus Marine Service Information.

275 **Financial support**

276 This study has been partly funded by the Mediterranean Copernicus Monitoring and Forecast Center (contract LOT  
277 REFERENCE: 21002L5-COP-MFC MED-5500 issued by Mercator Ocean) within the framework of Marine Copernicus  
278 Service.

279 **References**

280 **Batistić, M., Garić, R., & Molinero, J. C. (2014). Interannual variations in Adriatic Sea zooplankton mirror shifts in circulation**  
281 **regimes in the Ionian Sea. *Climate research*, 61(3), 231-240, 2014.**

282

283 Beg Paklar, G., Vilibić, I., Grbec, B., Matić, F., Mihanović, H., Džoić, T., et al.: Record-breaking salinities in the middle  
284 Adriatic during summer 2017 and concurrent changes in the microbial food web. *Prog. Oceanogr.* 185:102345. doi:  
285 10.1016/j.pocean.2020.102345, 2020.

286

287 Beyer, R., Krapp, M., and Manica, A.: An empirical evaluation of bias correction methods for palaeoclimate simulations, *Clim.*  
288 *Past*, 16, 1493–1508, <https://doi.org/10.5194/cp-16-1493-2020>, 2020.

289

290 Breitburg, D., Levin, L. A., Oschlies, A., Grégoire, M., Chavez, F. P., Conley, D. J., ... & Zhang, J.: Declining oxygen in the  
291 global ocean and coastal waters. *Science*, 359(6371), eaam7240, 2018.

292

293 Chiarini, M., Guicciardi, S., Angelini, S., Tuck, I. D., Grilli, F., Penna, P., ... & Martinelli, M.: Accounting for environmental  
294 and fishery management factors when standardizing CPUE data from a scientific survey: A case study for *Nephrops norvegicus*  
295 in the Pomo Pits area (Central Adriatic Sea). *PloS one*, 17(7), e0270703, 2022.

296

297 Civitarese, G., Gačić, M., Lipizer, M., & Eusebi Borzelli, G. L.: On the impact of the Bimodal Oscillating System (BiOS) on  
298 the biogeochemistry and biology of the Adriatic and Ionian Seas (Eastern Mediterranean). *Biogeosciences*, 7(12), 3987-3997.  
299 <https://doi.org/10.5194/bg-7-3987-2010>, 2010.

300

301 Conley, D. J., Björck, S., Bonsdorff, E., Carstensen, J., Destouni, G., Gustafsson, B. G., ... & Zillén, L.: Hypoxia-related  
302 processes in the Baltic Sea. *Environmental Science & Technology*, 43(10), 3412-3420, 2009.

303

304 Copin-Montégut, C. and Bégovic, M.: Distributions of carbonate properties and oxygen along the water column (0-2000 m)  
305 in the central part of the NW Mediterranean Sea (dyfamed site): Influence of winter vertical mixing on air-sea CO<sub>2</sub> and O<sub>2</sub>  
306 exchanges, *Deep. Res. Part II Top. Stud. Oceanogr.*, 49(11), 2049–2066, doi:10.1016/S0967-0645(02)00027-9, 2002.

307

308 Coppola, L., Legendre, L., Lefevre, D., Prieur, L., Taillandier, V. and Diamond Riquier, E.: Seasonal and inter-annual  
309 variations of dissolved oxygen in the northwestern Mediterranean Sea (DYFAMED site), *Prog. Oceanogr.*, 162(January), 187–  
310 201, doi:10.1016/j.pocean.2018.03.001, 2018.

311

312 Cossarini, G., Feudale, L., Teruzzi, A., Bolzon, G., Coidessa, G., Solidoro, C., Di Biagio, V., Amadio, C., Lazzari, P., Brosich,  
313 A. and Salon, S.: High-resolution reanalysis of the Mediterranean Sea biogeochemistry (1999-2019). *Frontiers in Marine*  
314 *Science*, 1537, <https://doi.org/10.3389/fmars.2021.741486>, 2021.

315

316 Cushman-Roisin, B., Gacic, M., Poulain, P. M., & Artegiani, A. (Eds.): *Physical oceanography of the Adriatic Sea: past,*  
317 *present and future.* Springer Science & Business Media, 2013.

318

319 Di Biagio, V., Salon, S., Feudale, L., and Cossarini, G.: Subsurface oxygen maximum in oligotrophic marine ecosystems:  
320 mapping the interaction between physical and biogeochemical processes, *Biogeosciences* 19, 5553–5574, ~~Discuss. [preprint]~~,  
321 <https://doi.org/10.5194/bg-2022-70>, in review <https://doi.org/10.5194/bg-19-5553-2022>, 2022.

322

323 Ekau, W., Auel, H., Pörtner, H. O., & Gilbert, D.: Impacts of hypoxia on the structure and processes in pelagic communities  
324 (zooplankton, macro-invertebrates and fish). *Biogeosciences*, 7(5), 1669-1699, 2013.

325

326 [Escudier, R., Clementi, E., Omar, M., Cipollone, A., Pistoia, J., Aydogdu, A., Drudi, M., Grandi, A., Lyubartsev, V., Lecci,](https://doi.org/10.25423/CMCC/MEDSEA_MULTIYEAR_PHY_006_004_E3R1_2020)  
327 [R., Cretí, S., Masina, S., Coppini, G., & Pinardi, N. Mediterranean Sea Physical Reanalysis \(CMEMS MED-Currents\) \(Version](https://doi.org/10.25423/CMCC/MEDSEA_MULTIYEAR_PHY_006_004_E3R1_2020)  
328 [1\) Data set. Copernicus Monitoring Environment Marine Service](https://doi.org/10.25423/CMCC/MEDSEA_MULTIYEAR_PHY_006_004_E3R1_2020)  
329 [\(CMEMS\). https://doi.org/10.25423/CMCC/MEDSEA\\_MULTIYEAR\\_PHY\\_006\\_004\\_E3R1\\_2020.](https://doi.org/10.25423/CMCC/MEDSEA_MULTIYEAR_PHY_006_004_E3R1_2020)

330

331 Escudier R., Clementi E., Cipollone A., Pistoia J., Drudi M., Grandi A., Lyubartsev V., Lecci R., Aydogdu A., Delrosso D.,  
332 Omar M., Masina S., Coppini G. and Pinardi N.: A High Resolution Reanalysis for the Mediterranean Sea. *Front. Earth Sci.*  
333 9:702285. <https://doi.org/10.3389/feart.2021.702285>, 2021.

334

335 Gačić, M., Civitarese, G., Miserocchi, S., Cardin, V., Crise, A., & Mauri, E.: The open-ocean convection in the Southern  
336 Adriatic: a controlling mechanism of the spring phytoplankton bloom. *Continental Shelf Research*, 22(14), 1897-1908, 2002.

337

338 [Gačić, M.; Borzelli, G.E.; Civitarese, G.; Cardin, V.; Yari, S.; Can internal processes sustain reversals of the ocean upper](https://doi.org/10.1029/2009JC005749)  
339 [circulation? The Ionian Sea example. \*Geophys. Res. Lett.\*, 37 \(9\) :L09608, DOI:10.1029/2009JC005749, 2010.](https://doi.org/10.1029/2009JC005749)

340

341 [Gačić, M.; Civitarese, G.; Eusebi Borzelli, G.L.; Kovačević, V.; Poulain, P.M.; Theocharis, A.; Menna, M.; Catucci, A.;](https://doi.org/10.1029/2011JC007280)  
342 [Zarokanellos, N.; On the relationship between the decadal oscillations of the northern Ionian Sea and the salinity distributions](https://doi.org/10.1029/2011JC007280)  
343 [in the eastern Mediterranean.; \*J. Geophys. Res. Oceans\*, 116, C12, https://doi.org/10.1029/2011JC007280, 2011.](https://doi.org/10.1029/2011JC007280)

344

345 [Gačić, M.; Ursella, L.; Kovačević, V.; Menna, M.; Malačič, V.; Bensi, M.; Negretti, M.E.; Cardin, V.; Orlić, M.; Sommeria,](https://doi.org/10.5194/os-17-975-2021)  
346 [J.; Barreto, R.V.; Viboud, S.; Valran, T.; Petelin, B.; Siena, G.; Rubino, A.; Impact of dense-water flow over a sloping bottom](https://doi.org/10.5194/os-17-975-2021)  
347 [on open-sea circulation: laboratory experiments and an Ionian Sea \(Mediterranean\) example. \*Ocean Sci.\*, 17, 975–996,](https://doi.org/10.5194/os-17-975-2021)  
348 [https://doi.org/10.5194/os-17-975-2021, 2021.](https://doi.org/10.5194/os-17-975-2021)

349

350 Garcia-Soto, C., Cheng, L., Caesar, L., Schmidtko, S., Jewett, E. B., Cheripka, A., Rigor I., Caballero A., Chiba S., Báez J.  
351 C., Zielinski T. and Abraham, J. P.: An overview of ocean climate change indicators: Sea surface temperature, ocean heat  
352 content, ocean pH, dissolved oxygen concentration, arctic sea ice extent, thickness and volume, sea level and strength of the  
353 AMOC (Atlantic Meridional Overturning Circulation). *Frontiers in Marine Science*.  
354 <https://www.frontiersin.org/article/10.3389/fmars.2021.642372>, 2021.

355

356 Gudmundsson, L., Bremnes, J. B., Haugen, J. E., & Engen-Skaugen, T.: Downscaling RCM precipitation to the station scale  
357 using statistical transformations—a comparison of methods. *Hydrology and Earth System Sciences*, 16(9), 3383-3390, 2012.

358

359 [Hersbach, H., Bell, B., Berrisford, P., Biavati, G., Horányi, A., Muñoz Sabater, J., Nicolas, J., Peubey, C., Radu, R., Rozum,](#)  
360 [I., Schepers, D., Simmons, A., Soci, C., Dee, D., Thépaut, J.-N.: ERA5 hourly data on single levels from 1959 to present.](#)  
361 [Copernicus Climate Change Service \(C3S\) Climate Data Store \(CDS\). \(Accessed on 6-3-2023\), 10.24381/cds.adbb2d47, 2018.](#)

362

363 Hopson, T. M., & Webster, P. J.: A 1–10-day ensemble forecasting scheme for the major river basins of Bangladesh:  
364 Forecasting severe floods of 2003–07. *Journal of Hydrometeorology*, 11(3), 618-641, 2010.

365

366 Jakob Themeßl, M., Gobiet, A. and Leuprecht, A.: Empirical-statistical downscaling and error correction of daily precipitation  
367 from regional climate models. *Int. J. Climatol.*, 31: 1530-1544. <https://doi.org/10.1002/joc.2168>, 2011.

368

369 Keeling, R. F., & Garcia, H. E.: The change in oceanic O<sub>2</sub> inventory associated with recent global warming. *Proceedings of*  
370 *the National Academy of Sciences*, 99(12), 7848-7853, 2002.

371

372 Kokkini Z., Mauri E., Gerin R., Poulain P.-M., Simoncelli S., Notarstefano G.: On the salinity structure in the South Adriatic  
373 as derived from float and glider observations in 2013–2016. *Deep-Sea Research Part II* 11 pp, 2019.

374

375 Kokkini Z., Notarstefano G., Poulain P.-M., Mauri E., Gerin R., Simoncelli S. (2018). In Von Schuckmann et al.: Unusual  
376 salinity pattern in the South Adriatic Sea. Copernicus Marine Service Ocean State Report 2018-09-08 - *Journal of Operational*  
377 *Oceanography*, 11:sup1, S1-S142, 2018.

378

379 Kress, N., & Herut, B.: Spatial and seasonal evolution of dissolved oxygen and nutrients in the Southern Levantine Basin  
380 (Eastern Mediterranean Sea): chemical characterization of the water masses and inferences on the N: P ratios. *Deep Sea*  
381 *Research Part I: Oceanographic Research Papers*, 48(11), 2347-2372, 2001.

382

383 Kwiatkowski, L., Torres, O., Bopp, L., Aumont, O., Chamberlain, M., Christian, J. R., ... & Ziehn, T.: Twenty-first century  
384 ocean warming, acidification, deoxygenation, and upper-ocean nutrient and primary production decline from CMIP6 model  
385 projections. *Biogeosciences*, 17(13), 3439-3470. <https://doi.org/10.5194/bg-17-3439-2020>, 2020.

386

387 Lipizer, M., Partescano, E., Rabitti, A., Giorgetti, A., & Crise, A.: Qualified temperature, salinity and dissolved oxygen  
388 climatologies in a changing Adriatic Sea. *Ocean Science*, 10(5), 771-797. <https://doi.org/10.5194/os-10-771-2014>, 2014.

389

390 [Malanotte-Rizzoli, P., Manca, B. B., d'Alcala, M. R., Theocharis, A., Brenner, S., Budillon, G., & Ozsoy, E. The Eastern](#)  
391 [Mediterranean in the 80s and in the 90s: the big transition in the intermediate and deep circulations. \*Dynamics of Atmospheres\*](#)  
392 [and \*Oceans\*, 29\(2-4\), 365-395, 1999.](#)  
393

394 Manca, B., Burca, M., Giorgetti, A., Coatanoan, C., Garcia, M. J., & Iona, A.: Physical and biochemical averaged vertical  
395 profiles in the Mediterranean regions: an important tool to trace the climatology of water masses and to validate incoming data  
396 from operational oceanography. *Journal of Marine Systems*, 48(1-4), 83-116, 2004.

397

398 [Manca, B., Ibello, V., Pacciaroni, M., Scarazzato, P., & Giorgetti, A. Ventilation of deep waters in the Adriatic and Ionian](#)  
399 [Seas following changes in thermohaline circulation of the Eastern Mediterranean. \*Climate Research\*, 31\(2-3\), 239-256, 2006.](#)  
400

401 Martellucci, R., Salon, S., Cossarini, G., Piermattei, V., & Marcelli, M.: Coastal phytoplankton bloom dynamics in the  
402 Tyrrhenian Sea: Advantage of integrating in situ observations, large-scale analysis and forecast systems. *Journal of Marine*  
403 *Systems*, 218, 103528, 2021.

404

405 Matear, R. J., Hirst, A. C., & McNeil, B. I.: Changes in dissolved oxygen in the Southern Ocean with climate  
406 change. *Geochemistry, Geophysics, Geosystems*, 1(11), 2000.

407

408 Mauri E, Menna M, Garić R, Batistić M, Libralato S, Notarstefano G, Martellucci R, Gerin R, Pirro A, Hure M, Poulain P-M.  
409 Recent changes of the salinity distribution and zooplankton community in the South Adriatic Pit, *Journal of Operational*  
410 *Oceanography*, Copernicus Marine Service Ocean State Report, Issue 5. 14 (sup1), pp.1-185,  
411 <https://doi.org/10.1080/1755876X.2021.1946240>, 2021.

412

413 [Mavropoulou, A. M., Vervatis, V. and Sofianos, S.: Dissolved oxygen variability in the Mediterranean Sea, \*J. Mar. Syst.\*,](#)  
414 [208\(March\), doi:10.1016/j.jmarsys.2020.103348, 2020.](#)  
415

416 Mella-Flores, D., Mazard, S., Humily, F., Partensky, F., Mahe, F., Bariat, L., et al.: Is the distribution of *Prochlorococcus* and  
417 *Synechococcus* ecotypes in the Mediterranean Sea affected by global warming? *Biogeosciences* 8, 2785–2804. doi:  
418 10.5194/bg-8-2785-2011, 2011.

419

420 Menna, M.; Reyes-Suarez, N.C.; Civitarese, G.; Gačić, M.; Poulain, P.-M.; Rubino, A.; Decadal variations of circulation in  
421 the Central Mediterranean and its interactions with the mesoscale gyres. *Deep Sea Res. Part II Top. Stud. Oceanogr.*, 164, 14-  
422 24, <https://doi.org/10.1016/j.dsr2.2019.02.004>, 2019.

423

424 [Menna M., Gačić M., Martellucci R., Notarstefano G., Fedele G., Mauri E., Gerin R., Poulain P.-M.: Climatic, decadal and](#)  
425 [interannual variability in the upper layer of the Mediterranean Sea using remotely sensed and in-situ data. Remote sensing,](#)  
426 [14, 1322. https://doi.org/10.3390/rs14061322, 2022a.](#)

427

428 Menna, M., Martellucci, R., Notarstefano, G., Mauri, E., Gerin, R., Pacciaroni, M., Bussani, A., Pirro, A., Poulain, P.-M. :  
429 Record-breaking high salinity in the South Adriatic Pit in 2020, ~~accepted by~~ Copernicus Marine Service Ocean State Report 6  
430 - Journal of Operational Oceanography, 2022**b**.

431

432 Mihanović, H., Vilibić, I., Šepić, J., Matić, F., Ljubešić, Z., Mauri, E., ... & Poulain, P. M.: Observation, Preconditioning and  
433 Recurrence of Exceptionally High Salinities in the Adriatic Sea. *Frontiers in Marine Science*, 8, 834.  
434 <https://doi.org/10.3389/fmars.2021.672210>, 2021.

435

436 Oesterwind, Daniel, Andrea Rau, and Anastasija Zaiko: Drivers and pressures—untangling the terms commonly used in marine  
437 science and policy. *Journal of environmental management* 181, 8-15, 2016.

438

439 Oeschlies, A., Schulz, K. G., Riebesell, U., & Schmittner, A.: Simulated 21st century's increase in oceanic suboxia by CO2-  
440 enhanced biotic carbon export. *Global Biogeochemical Cycles*, 22(4), 2008.

441

442 Oeschlies, A., Brandt, P., Stramma, L., & Schmidtko, S.: Drivers and mechanisms of ocean deoxygenation. *Nature Geoscience*,  
443 11(7), 467-473, 2018.

444

445 Querin, S., M. Bensi, V. Cardin, C. Solidoro, S. Bacer, L. Mariotti, F. Stel, and V. Malac'ic': Saw-tooth modulation of the  
446 deep-water thermohaline properties in the southern Adriatic Sea, *J. Geophys. Res. Oceans*, 121, 4585–4600,  
447 <https://doi.org/10.1002/2015JC011522>, 2016.

448

449 Pirro, A., Mauri, E., Gerin, R., Martellucci, R., Zuppelli, P., & Poulain, P. M.: New insights on the formation and breaking  
450 mechanism of convective cyclonic cones in the South Adriatic Pit during winter 2018. *Journal of Physical Oceanography*,  
451 2022.

452

453 Pitcher, G. C., Aguirre-Velarde, A., Breitburg, D., Cardich, J., Carstensen, J., Conley, D. J., ... & Zhu, Z. Y.: System controls  
454 of coastal and open ocean oxygen depletion. *Progress in Oceanography*, 197, 102613, 2021.

455

456 [Pörtner, H. O., Roberts, D. C., Masson-Delmotte, V., Zhai, P., Tignor, M., Poloczanska, E., & Weyer, N. M. The ocean and](#)  
457 [cryosphere in a changing climate. IPCC Special Report on the Ocean and Cryosphere in a Changing Climate. Cambridge](#)  
458 [University Press, Cambridge, UK and New York, NY, USA, 755 pp., <https://doi.org/10.1017/9781009157964>, 2019.](#)  
459

460 Reale, M., Cossarini, G., Lazzari, P., Lovato, T., Bolzon, G., Masina, S., Solidoro, C., and Salon, S.: Acidification,  
461 deoxygenation, nutrient and biomasses decline in a warming Mediterranean Sea, *Biogeosciences* [19](#), 4035–4065,  
462 <https://doi.org/10.5194/bg-19-4035-2022>, ~~Discuss. [preprint], <https://doi.org/10.5194/bg-2021-301>, in review, 2021.~~  
463

464 Riser, S. C. and Johnson, K. S.: Net production of oxygen in the subtropical ocean, *Nature*, 451(7176), 323–325,  
465 doi:10.1038/nature06441, 2008.  
466

467 [Rubino, A.; Gačić, M.; Bensi, M.; Kovačević, V.; Malačić, V.; Menna, M.; Negretti, M.E.; Sommeria, J.; Zanchettin, D.;](#)  
468 [Barreto, R.V.; et al. Experimental evidence of long-term oceanic circulation reversals without wind influence in the North](#)  
469 [Ionian Sea. Sci. Rep., 10, 1905, \[10.1038/s41598-020-57862-6\]\(https://doi.org/10.1038/s41598-020-57862-6\), 2020.](#)  
470

471 [Teruzzi, A., Di Biagio, V., Feudale, L., Bolzon, G., Lazzari, P., Salon, S., Coidessa, G., & Cossarini, G. Mediterranean Sea](#)  
472 [Biogeochemical Reanalysis \(CMEMS MED-Biogeochemistry, MedBFM3 system\) \(Version 1\) Data set. Copernicus](#)  
473 [Monitoring Environment Marine Service](#)  
474 [\(CMEMS\). \[https://doi.org/10.25423/CMCC/MEDSEA\\\_MULTIYEAR\\\_BGC\\\_006\\\_008\\\_MEDBFM3\]\(https://doi.org/10.25423/CMCC/MEDSEA\_MULTIYEAR\_BGC\_006\_008\_MEDBFM3\), 2021a.](#)  
475

476 [Teruzzi, A., Feudale, L., Bolzon, G., Lazzari, P., Salon, S., Di Biagio, V., Coidessa, G., & Cossarini, G. Mediterranean Sea](#)  
477 [Biogeochemical Reanalysis INTERIM \(CMEMS MED-Biogeochemistry, MedBFM3i system\) \(Version 1\) Data set.](#)  
478 [Copernicus Monitoring Environment Marine Service](#)  
479 [\(CMEMS\) \[https://doi.org/10.25423/CMCC/MEDSEA\\\_MULTIYEAR\\\_BGC\\\_006\\\_008\\\_MEDBFM3I\]\(https://doi.org/10.25423/CMCC/MEDSEA\_MULTIYEAR\_BGC\_006\_008\_MEDBFM3I\) \(accessed March 6,](#)  
480 [2023\), 2021b.](#)  
481

482 [Thiemeßl J., M., Gobiet, A. and Leuprecht, A. Empirical-statistical downscaling and error correction of daily precipitation from](#)  
483 [regional climate models. Int. J. Climatol., 31: 1530-1544. <https://doi.org/10.1002/joc.2168>, 2011.](#)  
484

485 Stramma, L., Schmidtko, S., Levin, L. A., & Johnson, G. C.: Ocean oxygen minima expansions and their biological impacts.  
486 *Deep Sea Research Part I: Oceanographic Research Papers*, 57(4), 587-595, 2010.  
487

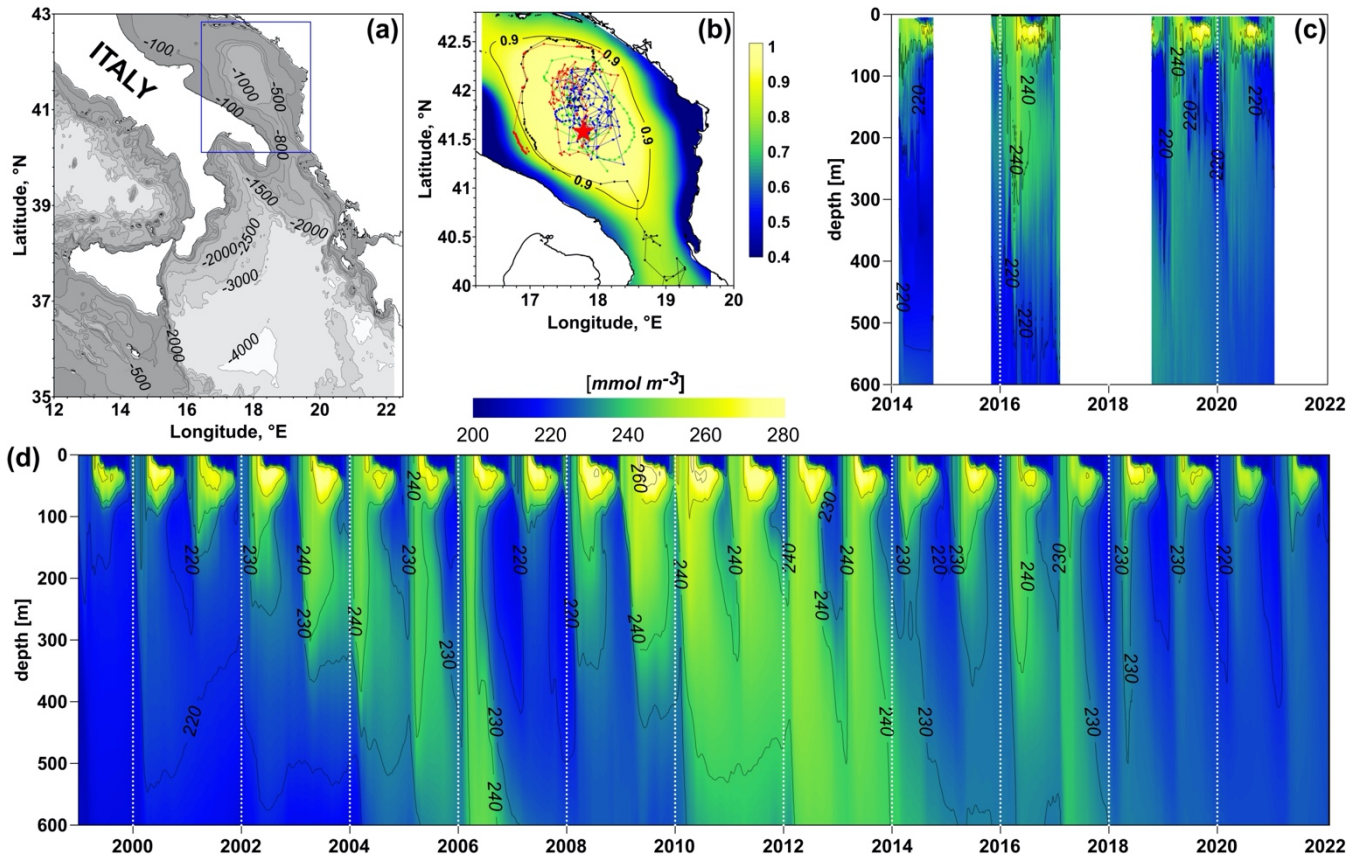
488 Thomson, Richard E., and William J. Emery. *Data analysis methods in physical oceanography*. Newnes, 2014.  
489

490 Vilibić, I., and Mihanović, H.: Observing the bottom density current over a shelf using an Argo profiling float, *Geophys. Res.*  
491 *Let.*, 40, 910–915, doi:[10.1002/grl.50215](https://doi.org/10.1002/grl.50215), 2013.

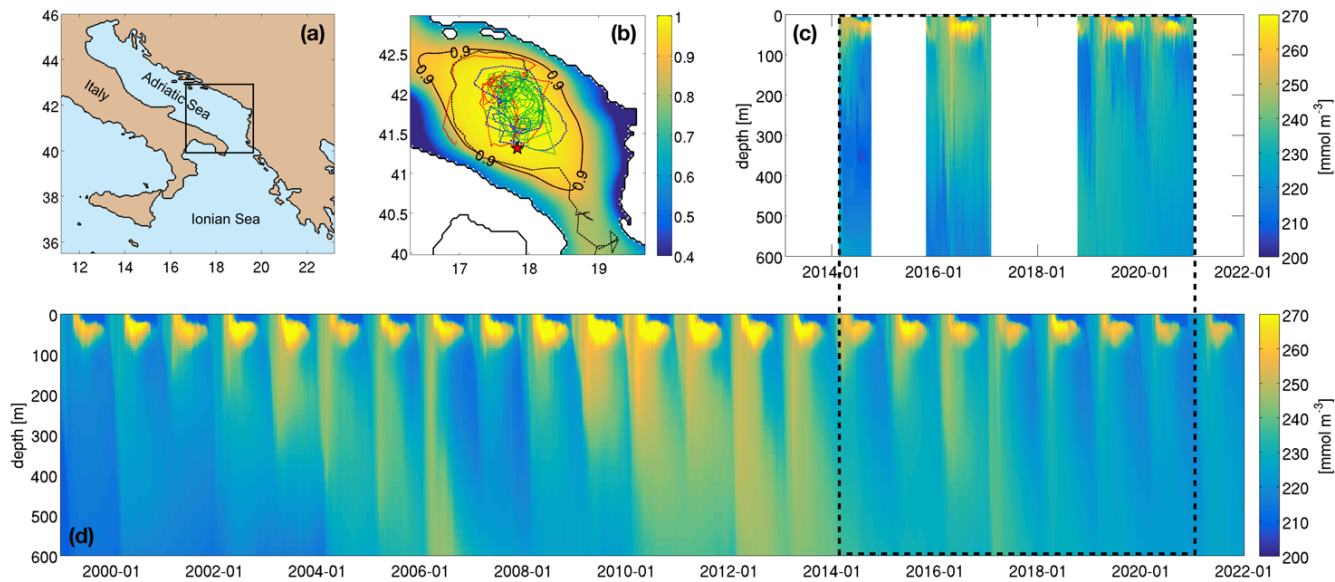
492

493 Yasunaka, S., Ono, T., Sasaoka, K., and Sato, K.: Global distribution and variability of subsurface  
494 chlorophyll a concentrations, *Ocean Sci.*, 18, 255–268, <https://doi.org/10.5194/os-18-255-2022>, 2022.

495

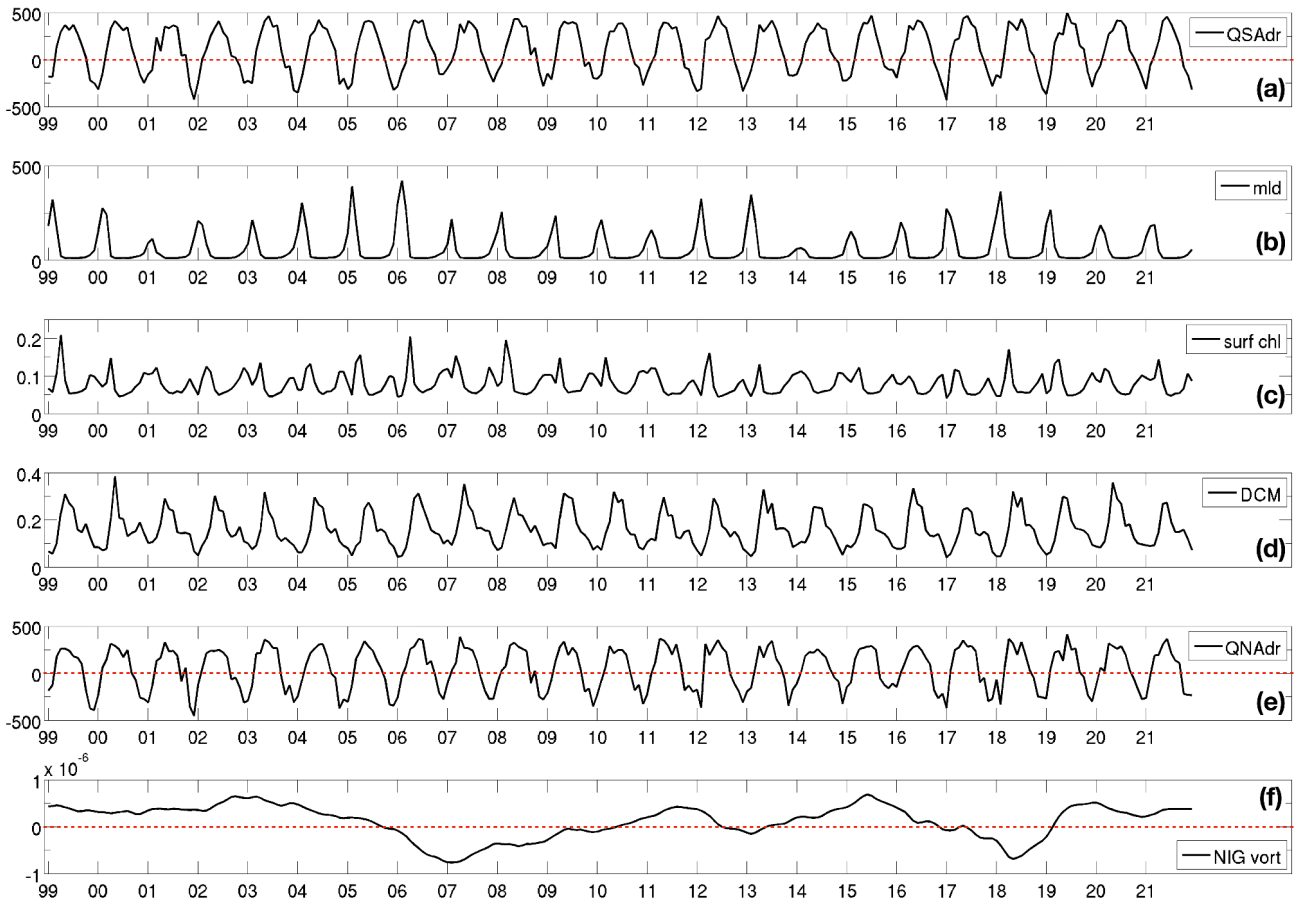


496

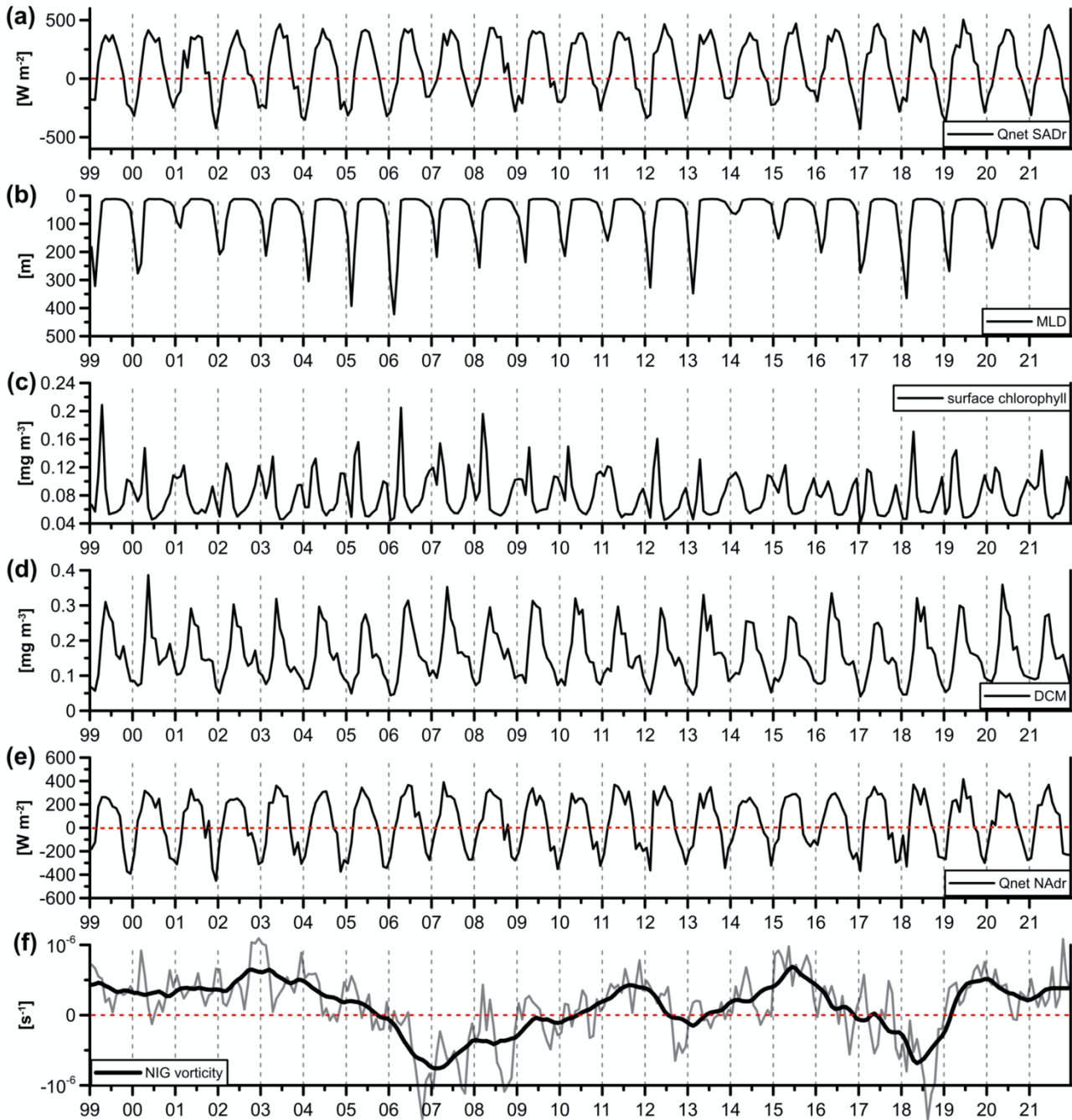


497

498 Figure 1: (a) Southern Adriatic area (black square) within Mediterranean Sea; (b) Cross-Autocorrelation map of surface oxygen,  
 499 nitrate and chlorophyll concentration provided by Copernicus biogeochemical reanalysis (Prod1, Table 1) in the Southern Adriatic  
 500 area with respect to the central point of the pit indicated by the red star; the black contour line delimits the area with cross-  
 501 autocorrelation equal or higher than 0.9; dashed lines indicate the trajectories of BGC-Argo floats (In Situ TAC data, Prod2) passing  
 502 the area. (c) Hovmöller diagrams of the dissolved oxygen concentration from In Situ TAC data (Prod2) within the area of cross-  
 503 autocorrelation equal to 0.9 (panel (b)). Data have been interpolated for sake of plot readability of the plot. (d) Hovmöller  
 504 diagrams of the dissolved oxygen concentration from Copernicus biogeochemical reanalysis (Prod1), spatially averaged within the  
 505 area of cross-autocorrelation equal to 0.9 (panel (a)) in 1999-2021 time period, after the bias correction procedure based on the In  
 506 Situ TAC data (Prod2).

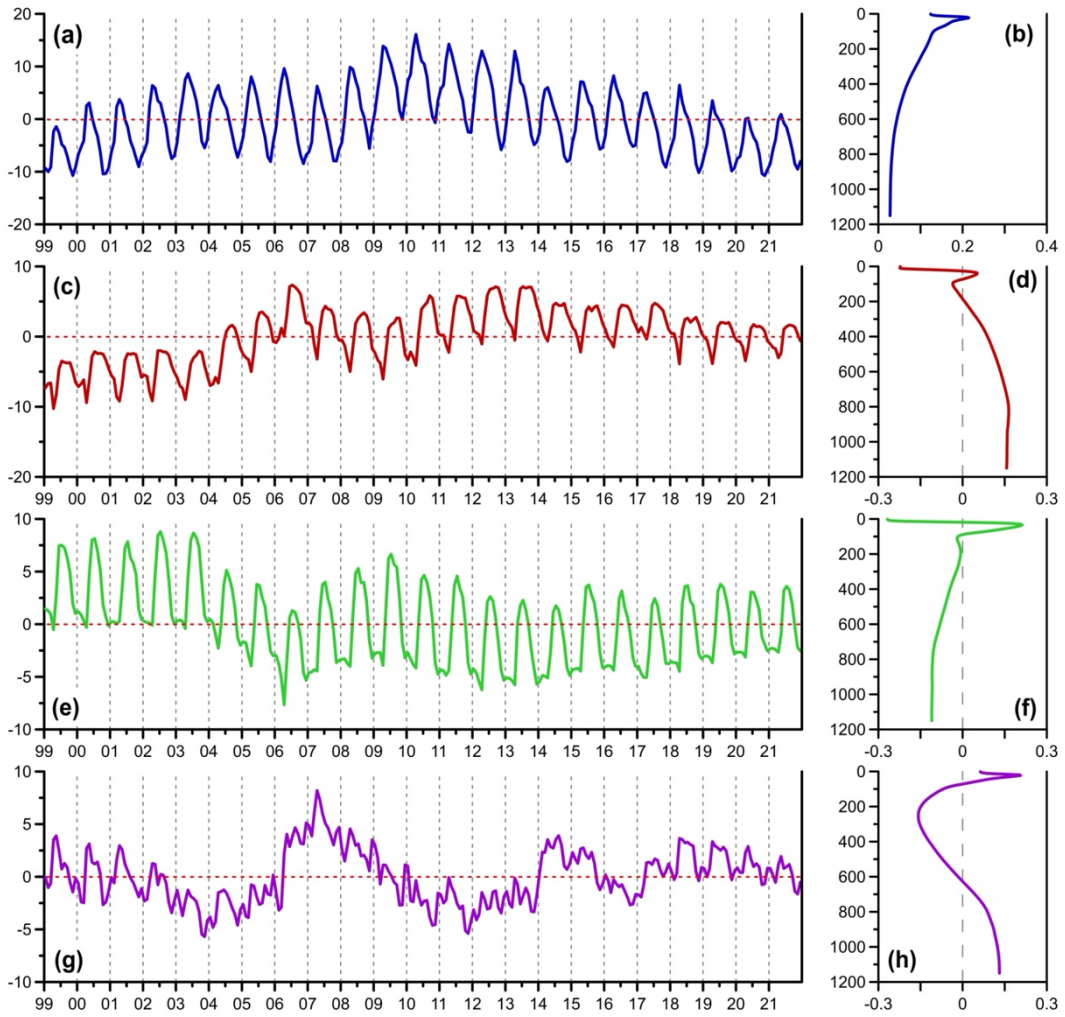


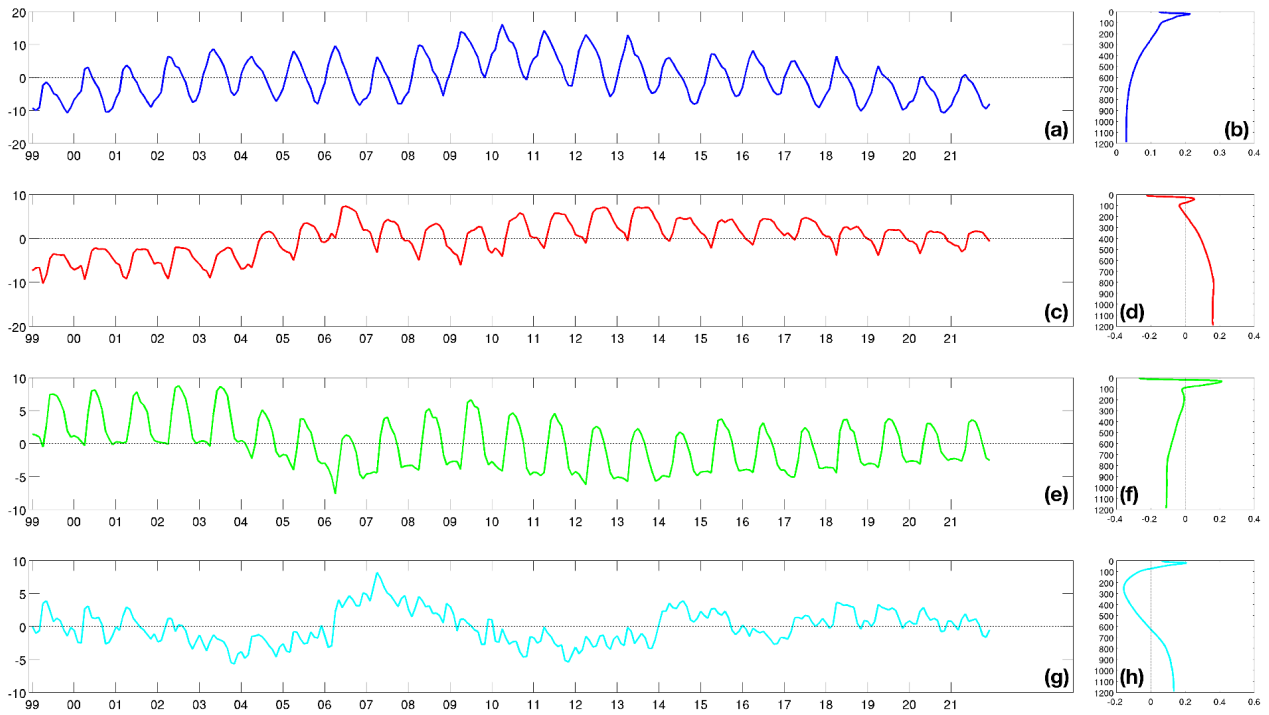
507



508

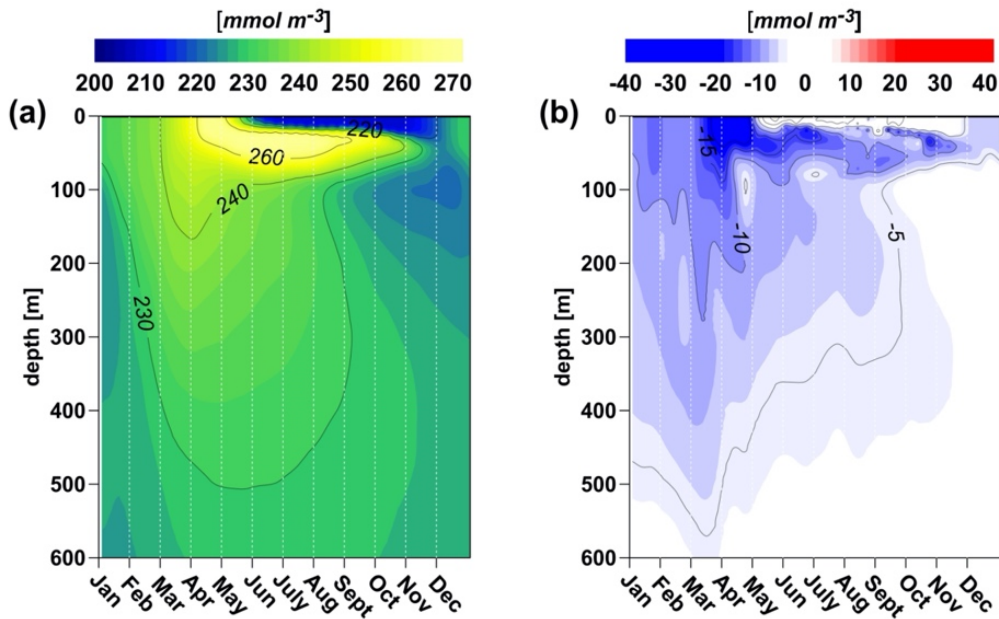
509 **Figure 2: Time series of the main forcing in the 1999-2021 time period: (a) net heat fluxes in SAdr (Prod6 in Table 1), in  $\text{W m}^{-2}$ ; (b)**  
 510 **mixed layer depth (Prod3), in  $\text{m}$ ; (c) surface chlorophyll concentration (Prod1), in  $\text{mg m}^{-3}$ ; (d) subsurface chlorophyll concentration**  
 511 **(30-80 m layer in which hosting deep chlorophyll maximum (DCM) is located, Prod1), in  $\text{mg m}^{-3}$ ; (e) net heat fluxes in NAdr (Prod6),**  
 512 **in  $\text{W m}^{-2}$ ; (f) NIG current vorticity (gray line) and de-seasonalized time series as obtained by applying a low-pass filter of 13 months**  
 513 **(black thick line), (Prod4 and Prod5), in  $\text{s}^{-1}$ .**



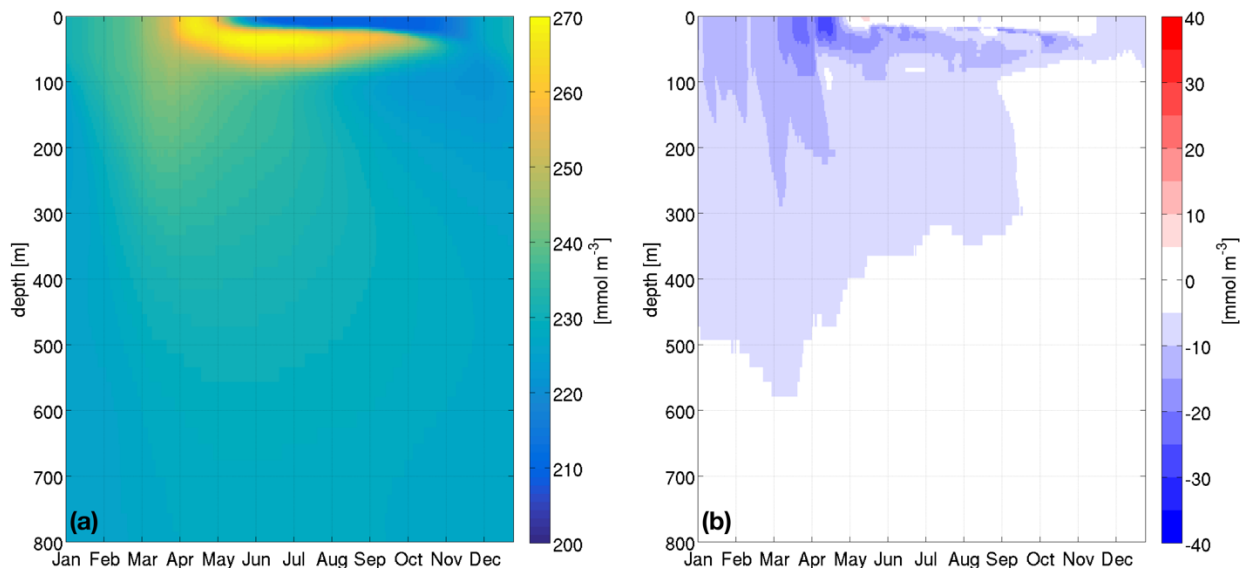


515

516 **Figure 3: First four EOF time series temporal (a, c, e, g) and vertical patterns (b, d, f, h) of the first four modes computed**  
 517 **on the bias-corrected dissolved oxygen concentration in the Southern Adriatic area shown in Fig. 1d. The explained variances of**  
 518 **the four modes are: 48.9%, 19.7%, 17.7% and 8.4%.**



519



520

521 **Figure 4: Hovmöeller diagrams of: climatological-mean over 1999-2020 of daily oxygen concentration computed from Copernicus**  
 522 **biogeochemical reanalysis (Prod1, Table 1) after the bias correction procedure based on the In Situ TAC data (Prod2) in 1999-2020**  
 523 **time-period (a) and anomaly in 2021 with respect to the 1999-2020 reference period (b).**

524

525

<u>Ref. no.</u> <b>Product id</b>	<u>Product Dataset-name &amp; type</u> <b>Type</b>	<u>DocumentationReferencee and</u> <b>dataset-doi</b>
<b>Prod1</b>	Copernicus Marine MEDSEA_MULTIYEAR_BGC_006_008 <u>Mediterranean Sea Biogeochemistry Reanalysis</u> <u>Mediterranean biogeochemical reanalysis</u>	Cossarini et al., (2021) <u>Dataset: Teruzzi et al., (2021a, 2021b)</u> <u><a href="https://doi.org/10.25423/CMCC/MEDSEA_MULTIYEAR_BGC_006_008_MEDBFM3">https://doi.org/10.25423/CMCC/MEDSEA_MULTIYEAR_BGC_006_008_MEDBFM3</a> (Accessed on 6-3-2023)</u> <u><a href="https://doi.org/10.25423/CMCC/MEDSEA_MULTIYEAR_BGC_006_008_MEDBFM3I">https://doi.org/10.25423/CMCC/MEDSEA_MULTIYEAR_BGC_006_008_MEDBFM3I</a> (Accessed on 6-3-2023)</u>
<b>Prod2</b>	Copernicus Marine INSITU_MED_NRT_OBSERVATIONS_013_035 <u>Mediterranean Sea-In-Situ Near Real Time Observations</u>	Copernicus Marine in situ TAC (2021). Copernicus Marine In Situ TAC quality information

	<del>Mediterranean in situ measurements</del>	document for Near Real Time In Situ products (QUID and SQO). <a href="https://doi.org/10.13155/75807">https://doi.org/10.13155/75807</a> (Accessed on 6-3-2023)
<del>Prod3</del>	Copernicus Marine MEDSEA_MULTIYEAR_PHY_006_004 <del>Mediterranean Sea Physics reanalysis</del> <del>Mediterranean physical reanalysis</del>	Escudier et al., (2021) <del>Dataset: Escudier et al., (2020)</del> <a href="https://doi.org/10.25423/CMCC/MEDSEA_MULTIYEAR_PHY_006_004_E3R1">https://doi.org/10.25423/CMCC/MEDSEA_MULTIYEAR_PHY_006_004_E3R1</a> (Accessed on 6-3-2023) <del><a href="https://doi.org/10.25423/CMCC/MEDSEA_MULTIYEAR_PHY_006_004_E3RH">https://doi.org/10.25423/CMCC/MEDSEA_MULTIYEAR_PHY_006_004_E3RH</a></del>
<del>Prod4</del>	Copernicus Marine SEALEVEL_EUR_PHY_L4_MY_008_068 <del>European Seas Gridded L 4 Sea Surface Heights And Derived Variables Reprocessed 1993 Ongoing</del> <del>European sea level gridded data based on altimetric measurements</del>	<a href="https://doi.org/10.48670/moi-00141">https://doi.org/10.48670/moi-00141</a> (Accessed on 6-3-2023)
<del>Prod5</del>	Copernicus Marine SEALEVEL_EUR_PHY_L4_NRT_OBSERVATIONS_008_060 <del>European Seas Gridded L 4 Sea Surface Heights And Derived Variables Nrt</del> <del>European sea level gridded data based on altimetric measurements</del>	<a href="https://doi.org/10.48670/moi-00142">https://doi.org/10.48670/moi-00142</a> (Accessed on 6-3-2023)
<del>Prod6</del>	Copernicus Climate ERA5 <del>Global climate and weather reanalysis</del> <del>Global climate and weather reanalysis</del>	Hersbach <del>at</del> el., 2018 <del>, H., Bell, B., Berrisford, P., Biavati, G., Horányi, A., Muñoz Sabater, J., Nicolas, J., Peubey, C., Radu, R., Rozum, I., Schepers, D., Simmons, A., Soci, C., Dee, D., Thépaut, J.-N. (2018): ERA5 hourly data on single levels from 1959 to present. Copernicus</del>

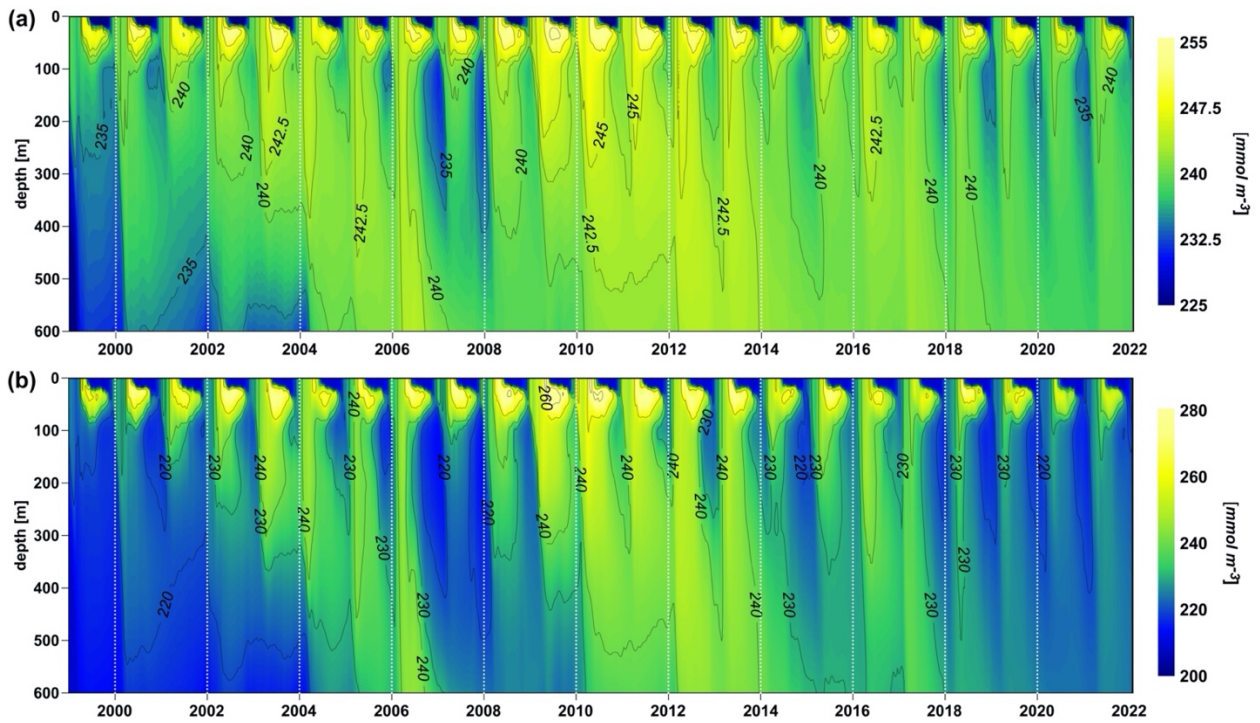
	Climate Change Service (C3S) Climate Data Store (CDS): (Accessed on 07-06-2022) <a href="https://doi.org/10.24381/cds.adbb2d47">https://doi.org/10.24381/cds.adbb2d47</a> (Accessed on 6-3-2023)
--	---

526 **Table 1: Product Datasets used in the present work, with reference and doi. Prod3 is a forcing for Prod1 and Prod6 is a forcing for**  
527 **Prod3. Complete references for the articles in Prod 1, and Prod 3 and Prod. 6 are reported in the bibliography.**

528  
529  
530

	mode 1	mode 2	mode 3	mode 4
<b>HFlux (SAdr)</b>	0.56	0.15	0.51	0.32
<b>MLD (SAdr)</b>	n.s.	-0.28	-0.41	-0.25
<b>surf chl (SAdr)</b>	n.s.	-0.41	-0.61	n.s.
<b>subsurface chl (SAdr)</b>	0.43	0.13	0.48	0.34
<b>Hflux NAdr (2-months lagged)</b>	n.s.	0.48	0.68	0.16
<b>NIG vorticity (Nlon)</b>	n.s.	-0.4036	0.26n.s.	-0.3744

531 **Table 2: Correlations between the first four temporal modes of EOFs of DO (first column in Figs. 3a,c,e,g) and the forcing fields**  
532 **(Fig. 2, with heat fluxes in the Northern Adriatic Sea time-lagged by two months). Not statistically significant correlations are**  
533 **identified by a significance level higher than 0.05 and indicated by “n.s.” acronym in the table.**

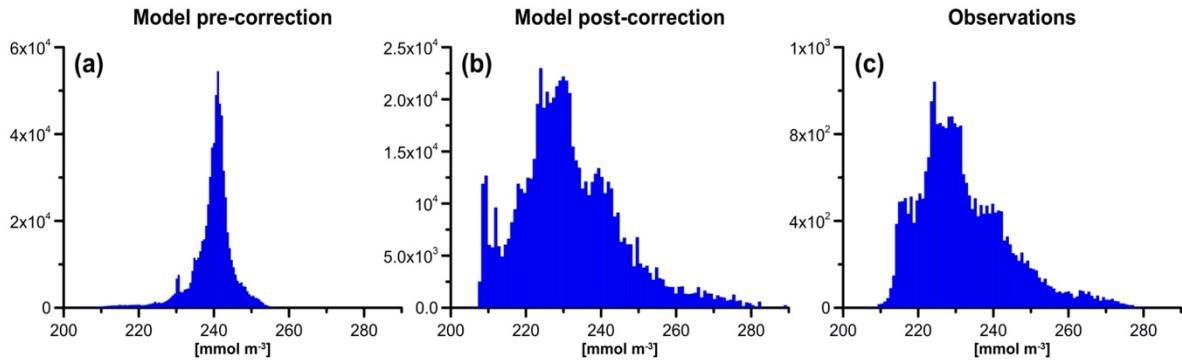


534

535 **Figure A1: Hovmöller diagram of the modelled oxygen concentrations spatially averaged within the area of autocorrelation equal**  
 536 **to 0.9 indicated in Fig 1b, before the bias correction by Quantile Mapping (a) and after the procedure (b).**

537

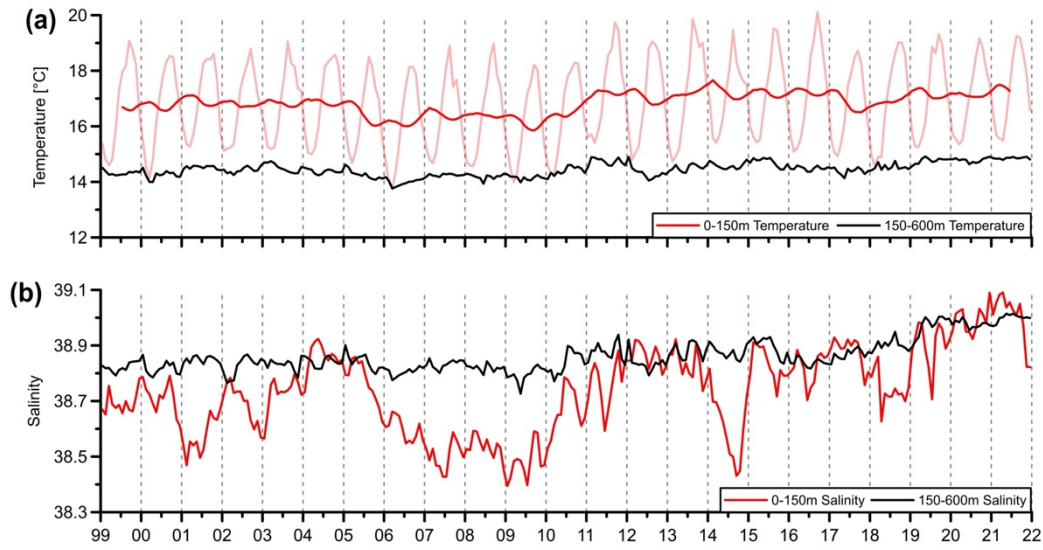
538



539

540 **Figure A2: Frequency histogram of modelled oxygen concentrations before the bias correction by Quantile Mapping (a) and after**  
 541 **the procedure (b), compared with BGC-Argo observations (c).**

542



543

544 **Figure B1: Time series of temperature (a) and salinity (b), averaged in the vertical layers 0 - 150 m (red lines) and 150-600 m (black**  
 545 **lines) of the Otranto Strait (39.8°N, 18.5° - 19.5° E) in the 1999-2021 time period. In the top panel, light red and dark red indicate**  
 546 **data before and after de-seasonalization, respectively. Data are provided by Copernicus physical reanalysis (Prod3, Table 1).**

547

548